ELSEVIER

Journal of Photochemistry and Photobiology A: Chemistry 149 (2002) 91–100

Journal of Photochemistry and Photobiology A:Chemistry

www.elsevier.com/locate/jphotochem

Photokinetic behaviour of bi-photochromic supramolecular systems Part 3. Compounds with chromene and spirooxazine units linked through ethane, ester and acetylene bridges

G. Favaro [a,*], D. Levi [b], F. Ortica [a], A. Samat [b], R. Guglielmetti [b], U. Mazzucato [a]

[a] *Dipartimento di Chimica, Università di Perugia, 06123 Perugia, Italy*

[b] *Faculté des Sciences de Luminy, Université de la Méditerranée, UMR CNRS 6114, 13288 Marseille Cedex 9, France*

Received 26 July 2001; received in revised form 31 October 2001; accepted 13 November 2001

Abstract

The photochemistry of four bi-photochromic (BiPh) compounds was investigated in toluene solution under steady state irradiation over a 20 °C temperature range. Three of these supermolecules are built up by two chromene moieties linked by a rigid acetylenic bridge (**1**) or flexible spacers, ethane (**3**) and ester (**4**); the other contains a chromene and a spirooxazine moieties linked by an ester bridge (**2**). Very efficient photo-colouration occurred upon UV irradiation at room temperature. Two of these systems (**1** and **2**) behaved as classical thermoreversible photochromic systems, while the other two compounds investigated (**3** and **4**) exhibited thermal and photochemical reversibility. This behaviour was attributed to formation of two (for **3**) and three (for **4**) photoproducts with different thermal and photochemical stability. By analytical and graphical treatments of the kinetic equations describing the dynamic behaviour of these photochromes, spectral, photochemical (quantum yields) and kinetic (rate constants and activation energies) parameters of these photochromic systems were determined.

Keywords: Photochromism; Chromenes; Spirooxazines; Bi-photochromes; Photokinetics; Reaction mechanism

1. Introduction

Spiropyrans, spirooxazines and chromenes have been largely investigated in the past because of their photochromic reactions which make them potentially suitable for different applications [1,2]. To increase colorability or tune the chromatic properties of these systems, a great number of substituted molecules have been synthesised and kinetically studied. Recently, attention has been turned to molecular structures containing two photochromic moieties linked through different molecular spacers thus leading to bi-photochromic (BiPh) supermolecules. First, compounds in which the two photochromes are joined through an ethenic bridge were kinetically studied [3,4]. These systems exhibited photochemical and dynamic properties different from those of the single components. They did not work as classical photochromes since they were not reversible, at least at room temperature. Visible photobleaching led to prevalent degradation. The peculiar behaviour of these bichromophoric molecules was attributed to the photoreactivity of the ethenic central bond which leads to cyclisation. This process is favoured by the *cis* configuration which is dominant in the synthesised compounds.

In this work, three BiPh molecules containing two 3H-naphtho[1,2-b]pyrans (chromene) moieties (**1**, **3** and **4**) and one containing both a spirooxazine and a chromene moieties (**2**) were investigated. The junction is rigid, like an acetylenic bridge (**1**), or flexible, like an ester (**2** and **4**) or an ethane bridge (**3**). In **1**, the acetylenic bridge is between the position 8 of the two 3,3-diphenyl-3H-naphtho[2,1-b]pyran units. In **2**, the ester bridge joins the position 8 of the naphthopyran to the position 5′ of the spirooxazine, while in **4** it joins positions 5 and 8 of the two naphthopyran moieties. In **3**, the ethane bridge is between the position 5 of the naphthopyran units (Scheme 1).

Interest in these compounds is two-fold. First, their colourability is expected to be improved, compared with the single molecule, due to the presence of two photochromic units. Secondly, their colour may be tuned by changing the two photochromes and extended over the whole visible spectrum when they are different, e.g. a chromene and a spirooxazine, which exhibit colouration in the 450 and 600 nm regions, respectively.

This study is aimed at understanding the photochemical and kinetic behaviour of the four compounds by determining

* Corresponding author. Fax: +39-075-585-5598.
E-mail address: favaro@phch.chm.unipg.it (G. Favaro).

1010-6030/02/$ – see front matter
PII: S1010-6030(01)00638-4

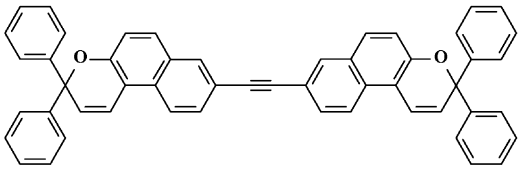

1

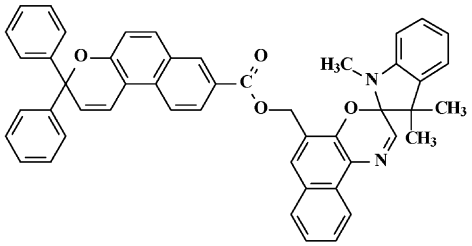

2

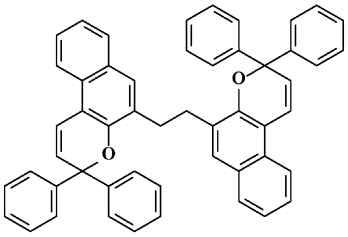

3

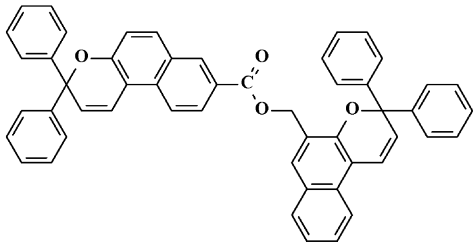

4

Scheme 1.

the reaction quantum yield(s) Φ, the molar absorption coefficient of the coloured form(s) ε, and the rate of the thermal back reaction k_Δ, which puts a limit to the amount of colourless form that is photoconvertible under steady irradiation.

An exhaustive view of the photokinetic behaviour of **1** and **2**, which act as classical thermoreversible photochromes, was achieved by applying rigorous photokinetic treatments to results obtained under continuous irradiation over a 20° C temperature range. For the other two molecules (**3** and **4**), the photoreaction leads to two/three different products, characterised by different thermal and photochemical stability. Information on the reaction mechanism and kinetics was obtained by approximate photokinetic methods.

2. Experimental

2.1. Materials

The supermolecules studied here were synthesised by the methods described in [5]. All measurements were carried out in toluene (Uvasol Fluka), used without further purification.

2.2. Apparatus and experimental conditions

Absorption spectra were recorded on a HP 8453 diode-array spectrophotometer. The irradiation of the sample (1 cm cell path, 1 cm^3 of solution) was carried out in the spectrophotometer holder at a right angle to the monitoring beam, using a fibre-optic system. The irradiation wavelengths were selected from the emission of a 75 W Xe lamp filtered by a monochromator (Jobin-Yvon H10 UV) in correspondence of an isosbestic point in order not to change the total absorbance during irradiation. The radiation intensity, typically of the order of 10^{-7} Einstein $dm^{-3}\,s^{-1}$, was determined at each wavelength using potassium ferrioxalate actinometry. The sample concentrations were of the order of 2×10^{-5} to 5×10^{-5} mol dm^{-3}. The photoreaction was followed, under stationary irradiation, at the absorption maximum wavelength of the coloured form up to photostationary state attainment over a 20 °C temperature range. An Oxford Instruments cryostat was used for the temperature control.

The kinetics of the thermal ring-closure reaction was recorded following the colour-bleaching of the irradiated solution immediately after the removal of the irradiating source. The activation energies of the thermal back reactions, along with the frequency factors, were determined from Arrhenius plots. An uncertainty of about 10% was evaluated for the activation energy, while the frequency factor was affected by more than 50% uncertainty.

With compounds **3** and **4**, a residual visible absorbance was observed, which faded under irradiation with visible light. The photobleaching reaction was kinetically followed by the decrease of absorbance in the visible spectral region.

3. Results and discussion

The study was carried out under steady irradiation, after preliminary determination of the spectral region where the colour band appeared and of the suitable temperature ranges. All BiPh molecules examined showed reversible photocolouration under irradiation with UV light. Results for compounds **1** and **2** will be presented together since the same kinetic approach was used.

$$\text{BiPh} \underset{\Delta}{\overset{h\nu}{\rightleftharpoons}} \text{C}$$

Scheme 2.

3.1. Compounds **1** and **2**

The acetylene-bridged compound (**1**) and the mixed chromene–spirooxazine compound (**2**) exhibit the thermoreversible behaviour shown in Scheme 2. Both of them are colourless and become coloured under UV irradiation. The absorption spectra of the closed forms lie at $\lambda \leq 390$ nm and show bands with maxima at 309 nm ($\varepsilon_{max} = 53{,}000\ dm^3\ mol^{-1}\ cm^{-1}$) and 348 nm ($\varepsilon_{max} = 30{,}000\ dm^3\ mol^{-1}\ cm^{-1}$) for **1,** and at 323 nm ($\varepsilon_{max} = 13{,}000\ dm^3\ mol^{-1}\ cm^{-1}$) for **2**.

The coloured form of **1**, obtained upon UV irradiation, exhibits a broad band centred at 485 nm. The spectra of the colourless and coloured forms of **1** are shown in Fig. 1.

Upon irradiation of **2**, two bands are observed in the visible region, $\lambda_{max} = 444$ and 608 nm. The spectra of the colourless and coloured forms of **2** are shown in Fig. 2. The two absorption regions are characteristic of the coloured forms of the open chromene moiety ($\lambda_{max} = 444$ nm) [6,7] and of the spirooxazine moiety ($\lambda_{max} = 608$ nm) [8,9], respectively. The colour-forming and colour-bleaching kinetics were followed on the colour maxima, 485 nm for **1** and both 444 and 608 nm for **2**. They were well fitted to monoexponential functions.

The rate constant of the thermal bleaching reaction k_Δ was determined from Eq. (1),

$$A_C = A_C^\infty\, e^{-k_\Delta t} \tag{1}$$

where A_C is the instantaneous absorbance of the metastable photoproduct C, and A_C^∞ its absorbance at the photostationary state. The activation energy was determined from Arrhenius plots using k_Δ values measured in the 255–280 K temperature range. The activation energy of the thermal bleaching of **1** was 67 kJ mol^{-1}.

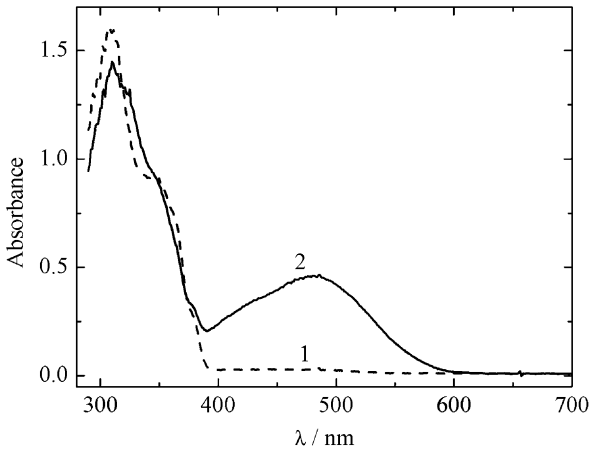

Fig. 1. Absorption spectra of **1** before irradiation (1) and at the photostationary state (2) in toluene; 3×10^{-5} mol dm^{-3}, at 255 K.

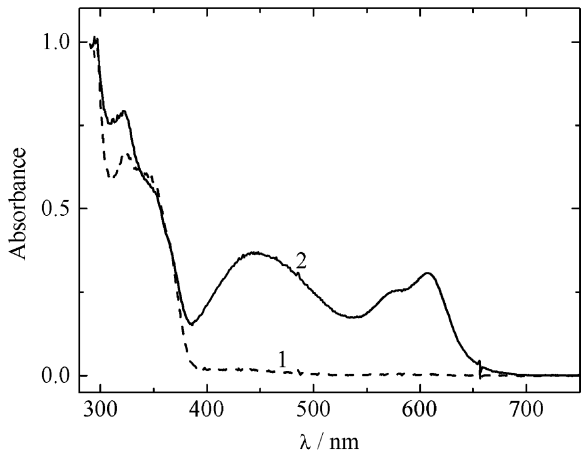

Fig. 2. Absorption spectra of **2** before irradiation (1) and at the photostationary state (2) in toluene; 3×10^{-5} mol dm^{-3}, at 255 K.

For **2**, the rate parameters obtained at both wavelengths were similar: at 280 K, $k_\Delta = 0.033$ and 0.027 s^{-1} at 444 and 608 nm, respectively. Also, the difference between the activation energies, determined at the two wavelengths in the 260–280 K temperature range, was within the experimental uncertainty (66 and 69 kJ mol^{-1}, at 444 and 608 nm, respectively).

For the reaction quantum yield determinations, photostationary and photokinetic methods were applied. Based on Scheme 2, the colour-forming kinetics is described by Eq. (2), where I_{BiPh} is the intensity of the light absorbed by BiPh, Φ the reaction quantum yield and k_Δ the rate constant of the thermal bleaching.

$$\frac{d[C]}{dt} = I_{BiPh}\Phi - k_\Delta[C] \tag{2}$$

In terms of the absorbance of C at the analysis wavelengths, the rate of the colour-forming process is expressed by Eq. (3), where $F = (1 - 10^{-A'})/A'$ is the photokinetic factor [10,11] (A' is the total absorbance at the irradiation wavelength), ε_{BiPh} is the molar absorption coefficient of the reactant at λ_{exc} and $[BiPh]_0$ is the initial concentration.

$$\frac{dA_C}{dt} = \varepsilon_C \Phi I_{BiPh} - k_\Delta A_C = \varepsilon_C \Phi I^0 F \varepsilon_{BiPh}[BiPh]_0 - (\Phi I^0 F \varepsilon_{BiPh} + k_\Delta) A_C \tag{3}$$

By using Eq. (3), alternative strategies were applied to determine Φ. For **2** this determination was carried out on both the chromene (Φ_{CHR}) and the spirooxazine (Φ_{SPO}) colour bands. The methods used to determine ε_C and Φ were:

(i) The integration method [11], which is based on the comparison of the parameters (A_C^∞ and α), obtained by graphical fit to a monoexponential function (Eq. (4)) of the experimental absorbance/time data sets and the integrated rate equation (Eq. (5)). This integration is only feasible if the photokinetic factor F is a time-independent parameter, i.e when irradiation is

carried out at an isosbestic point (373 nm for **1** and 337 nm for **2**).

$$A_C = A_C^{\infty}(1 - e^{-\alpha t}) \quad (4)$$

$$A_C = \frac{\varepsilon_C \Phi I^0 F \varepsilon_{BiPh}[BiPh]_0}{\Phi I^0 F \varepsilon_{BiPh} + k_\Delta}\left(1 - e^{-(\Phi I^0 F \varepsilon_{BiPh} + k_\Delta)t}\right) \quad (5)$$

Eq. (4) describes the experimental variation of the absorbance of C with time. In the exponent, α behaves like a rate coefficient and is the driving force for photoproduct accumulation under steady irradiation. The interpolation procedure of the experimental absorbance versus time data to this equation leads to the determination of the two parameters A_C^{∞} and α. By comparing Eqs. (4) and (5), the fitting parameters can be related to the photochemical and kinetic parameters through Eqs. (6) and (7), that allow Φ and ε_C to be determined.

$$A_C^{\infty} = \frac{\varepsilon_C \Phi I^0 F \varepsilon_{BiPh}[BiPh]_0}{\Phi I^0 F \varepsilon_{BiPh} + k_\Delta} \quad (6)$$

$$\alpha = \Phi I^0 F \varepsilon_{BiPh} + k_\Delta \quad (7)$$

(ii) The initial rate method [12] is based on the assumption that, initially, the absorbance increases linearly with time (constant colour-forming rate), since the bleaching process is negligible and the light absorbed by the reactant can be considered constant (Eq. (8)). The $\varepsilon_C\Phi$ product is obtained by dividing the initial slope of the ΔA_C versus Δt diagram by $I_{BiPh} = I^0(1 - 10^{-A'})$.

$$\frac{\Delta A_C}{\Delta t} = I_{BiPh}\varepsilon_C\Phi \quad (8)$$

(iii) The photokinetic method allows the $\varepsilon_C\Phi$ value to be obtained from the linear plot of dA_C/dt versus A_C (Eq. (3)), from both the intercept and slope [13].

(iv) The photostationary method [14] is based on the graphical treatment of Eq. (9), which represents linear relationship of $1/A_C^{\infty}$ versus k_Δ, if F can be assumed to be a constant (irradiation at an isosbestic point). This equation allows ε_C to be obtained from the intercept and Φ from the intercept to slope ratio. An example of data-treatment according to the photostationary method (Eq. (9)) is shown in Fig. 3.

$$\frac{1}{A_C^{\infty}} = \frac{1}{\varepsilon_C[BiPh]_0} + \frac{k_\Delta}{\Phi I^0 \varepsilon_{BiPh} F}\frac{1}{\varepsilon_C[BiPh]_0} \quad (9)$$

While all these methods gave well reproducible $\varepsilon_C\Phi$ values, the separate determination of ε_C, possible only by methods (i) and (iv), was the main source of uncertainty also in the Φ-value.

The estimated parameters obtained by the different approaches were: $\Phi = 0.45 \pm 0.05$ and $\varepsilon_C = 23{,}000 \pm 3000\,dm^3\,mol^{-1}\,cm^{-1}$ for **1**. For **2**, by using the three first approaches, comparable values were obtained. With the photostationary method, the values obtained for Φ_{CHR} and Φ_{SPO} showed some deviations, due to the uncertainty on the ε_C extrapolation. The molar absorption coefficients determined at λ_{max} of the two colour bands ($\varepsilon_{444} = 27{,}500 \pm 3000\,dm^3\,mol^{-1}\,cm^{-1}$ and $\varepsilon_{608} = 40{,}000 \pm 4000\,dm^3\,mol^{-1}\,cm^{-1}$) were of the order of magnitude expected for an open chromene form [6] and an open spirooxazine form [14–16], respectively. Due to the uncertainty on the molar absorption coefficients, the Φ_{CHR} and Φ_{SPO} values are affected by rather large errors ($\Phi_{CHR} = 0.20 \pm 0.03$ and $\Phi_{SPO} = 0.09 \pm 0.02$).

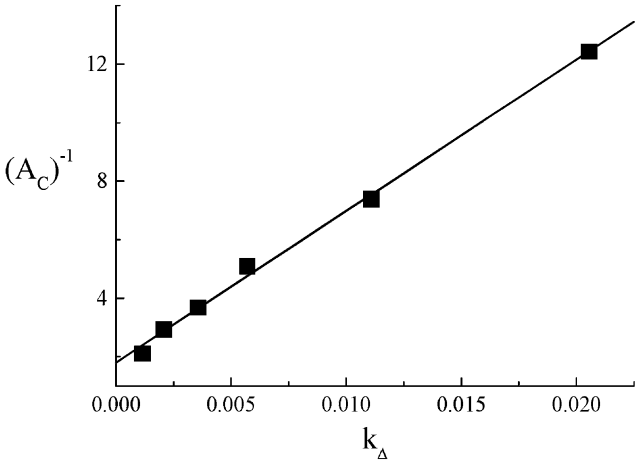

Fig. 3. Plot according to the photostationary method for Φ and ε determination (Eq. (9)), applied to **1**; 3×10^{-5} mol dm^{-3} toluene solution.

All parameters obtained for these two molecules are reported in Table 1 and compared with some literature values for the single photochromic moieties. While the agreement is good for the molar absorption coefficients, there are notable differences in the quantum yield values. However, it should be considered that the Φ-values reported in the literature for spirooxazine range from 0.19 [17] to 0.9 [18], due not only to the different measurement conditions but also to the intrinsic difficulty of measuring the formation quantum yield of a metastable species.

3.2. Compounds 3 and 4

These two molecules showed a photochemical behaviour typical of chromenes. A complex photochemistry occurred whereby the reactant **3** produced two coloured forms, one thermoreversible (C1) and the other photoreversible (C2), whereas **4** yielded three coloured forms, two thermoreversible (C1 and C2) and the other photoreversible (C3). The non-unique photoproduct formation was revealed by the bi-exponential increase of the colour band, Eq. (10), and by the occurrence of both thermal and photochemical bleaching. In Eq. (10), A is the sum of the individual absorbances of the two photoproducts at the maximum wavelength in the visible region, while B, C, α and β are fitting parameters.

$$A = B(1 - e^{-\alpha t}) + C(1 - e^{-\beta t}) \quad (10)$$

Table 1
Spectral and kinetic parameters obtained from the photokinetic study of **1** and **2** in toluene solution[a]

	1	**2**	
λ_{max} (nm)	480	444 (422 [6])	608 (592 [8], 601 [9], 585 [14])
λ_{exc} (nm)	373	337	
ε_{max} ($dm^3\,mol^{-1}\,cm^{-1}$)	23000	27500 (16000 [6])	40000 (31000 [8], 38000 [14])
Φ	0.45	0.20 (0.9 [6])	0.09 (0.23 ± 0.1 [8], 0.41 [14], 0.19 [17], 0.9 [18])
$k_{\Delta(280)}$ (s^{-1})	0.020	0.033	0.027
$k_{\Delta(298)}$ (s^{-1})	0.11	0.17	0.18
E_a ($kJ\,mol^{-1}$)	67.5	66	69
A (s^{-1})	1.6×10^{11}	7×10^{10}	2×10^{11}

[a] Literature data from [6,14] are in MCH.

The thermal bleaching processes, described by monoexponential and bi-exponential functions for **3** and **4**, respectively, left a residual absorption (A^{∞}_{C2} for **3** and A^{∞}_{C3} for **4**) which increased by decreasing temperature. These residues bleached under visible irradiation with the monoexponential trends described by Eq. (11), where the exponential coefficient γ contains experimental (the intensity of the excitation light) and intrinsic (photoreaction quantum yield and molar absorption coefficients at the analysis and excitation wavelengths) parameters of the system.

$$A_{C2} = A^{\infty}_{C2}\,e^{-\gamma t} \quad (11a)$$

$$A_{C3} = A^{\infty}_{C3}\,e^{-\gamma t} \quad (11b)$$

The rates of photobleaching are given by equations of the type of Eq. (12) (for C2 as an example), where A'_{C2} is the absorbance at the irradiation wavelength. Obviously, both A_{C2} and A'_{C2} are time-dependent variables.

$$\frac{-dA_{C2}}{dt} = I_{C2}\Phi_{-C2}\varepsilon_{C2} = I^0\Phi_{-C2}\varepsilon_{C2}(1 - 10^{-A'_{C2}}) \quad (12)$$

From Eq. (12), the product of the quantum yield of photobleaching and the molar absorption coefficient at the analysis wavelength ($\Phi_{-C2}\varepsilon_{C2}$) could be determined by plotting the experimental rate, $-dA_{C2}/dt$, against $10^{-A'_{C2}}$.

Considering that the differences between **3** and **4** are due to different reaction mechanisms, they will be separately described in more detail.

3.3. Compound 3

For compound **3**, the absorption spectrum of the colourless form is the typical one of 5,6-benzochromenes [6], showing two vibronically structured electronic transitions between 300 and 400 nm [λ_{max} (nm)/ ε_{max} ($dm^3\,mol^{-1}\,cm^{-1}$) = 309/18,500, 323/24,200, 348/16,600, 361/16,300]. The molar absorption coefficients are approximately double those of the single molecule. Both spectral shape and intensity indicate that the two photochromic moieties are substantially independent. This result is quite normal considering that the two moieties are joined by the non-conjugating –CH_2–CH_2– bridge. Excitation was carried out at an isosbestic point (365 nm). The coloured form showed a broad absorption band within 380 and 550 nm, with the maximum at 431 nm. The spectra at 275 K of the colourless non-irradiated solution and of the coloured solution at the photostationary state are shown in Fig. 4.

The thermal bleaching, studied in the 275–300 K temperature range, was described by a monoexponential function (Eq. (13)); the activation energy, determined by the Arrhenius plot, was 64 $kJ\,mol^{-1}$. The residual absorption (A^{∞}_{C2}), present after thermal bleaching, increased as temperature decreased.

$$A = A^{\infty}_{C1}\,e^{-k_{\Delta}t} + A^{\infty}_{C2} \quad (13)$$

This residue represents amounts from 7% (300 K) to 12% (275 K) of the total absorbance. Assuming that the absorption coefficients for C1 and C2 are similar, this means that the thermostable species is only a small fraction of the total reaction products. By subtracting the residue A^{∞}_{C2} from the total absorbance at the photostationary state, the photostationary absorbance of the thermally bleached product, A^{∞}_{C1}, was obtained. The latter data, that are reported in Table 2 together with the thermal bleaching constant at various temperatures, were treated according to the photostationary method (Eq. (9), correlation coefficient 0.998). The results obtained were: $\varepsilon = 30{,}100 \pm 3500\,dm^3\,mol^{-1}\,cm^{-1}$, from the intercept, and $\Phi_{C1} = 0.19 \pm 0.02$ from the intercept-to-slope ratio. The initial rate method (Eq. (8)) was also applied, assuming

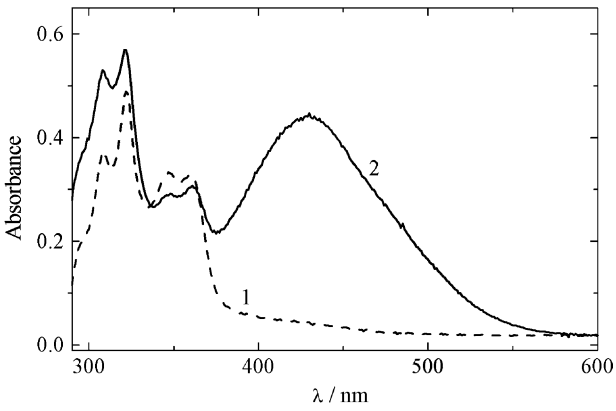

Fig. 4. Absorption spectra of **3** before irradiation (1) and at the photostationary state (2) in toluene solution; $3 \times 10^{-5}\,mol\,dm^{-3}$, at 275 K.

Table 2
Photostationary absorbance (A^{∞}) at the wavelength maximum of the colour band, thermal bleaching constant (k_{Δ}) and residual absorption (A^{∞}_{C2}) after thermal bleaching of **3** in 2×10^{-5} mol dm^{-3} toluene solution at various temperatures[a]

T (K)	A^{∞}	k_{Δ} (s^{-1})	A^{∞}_{C2}	A^{∞}_{C1}	$(\Phi_{C1}\varepsilon_{C1})_{\text{initial rate}}$ (dm^3 mol^{-1} cm^{-1})	$\varepsilon_{C1}\Phi_{C1} + \varepsilon_{C2}\Phi_{C2}$ (dm^3 mol^{-1} cm^{-1})
300	0.0830	0.0251	0.0057	0.0773	4421	6075
295	0.1239	0.0168	0.0111	0.1128	5150	6511
290	0.1797	0.0110	0.0209	0.1588	4920	6114
285	0.2586	0.0065	0.0352	0.2234	5200	6423
280	0.3159	0.0041	0.0432	0.2727	4770	5819
275	0.4130	0.0025	0.0546	0.3584	4800	5832

[a] $A^{\infty}_{C1} = A^{\infty} - A^{\infty}_{C2}$ is the photostationary absorbance of the thermo-bleachable photoproduct; $(\Phi_{C1}\varepsilon_{C1})_{\text{initial rate}}$ was obtained from Eq. (8) and $\varepsilon_{C1}\Phi_{C1} + \varepsilon_{C2}\Phi_{C2}$ from Eq. (15).

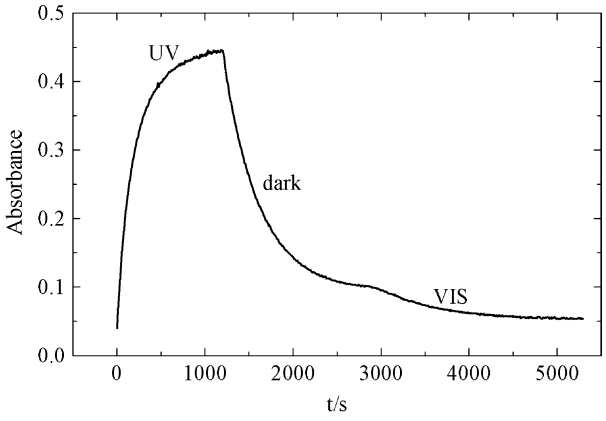

Fig. 5. Colour-forming and colour-bleaching (both thermal and photochemical) kinetics of **3** in toluene at 275 K.

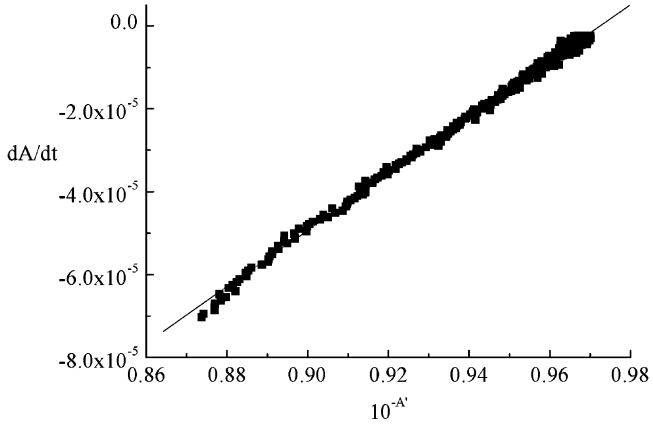

Fig. 6. Photobleaching absorbance data of **3** treated according to Eq. (12).

that the amount of C2 was initially negligible. The results supported this hypothesis, since the product $\varepsilon_{C1}\Phi_{C1}$ obtained (4900 ± 400 dm^3 mol^{-1} cm^{-1}) was wholly compatible with the above parameters.

Upon visible irradiation ($\lambda_{exc} = 431$ nm), the photobleaching was complete. An example of the kinetic profile, under UV irradiation, in the dark and under visible irradiation, followed at the colour band maximum ($\lambda_{analysis} = 431$ nm) at 275 K, is shown in Fig. 5. The kinetics of photobleaching fitted to a monoexponential function (Eq. (11)). The pre-exponential and exponential factors are reported in Table 3. The difference in the A^{∞}_{C2} values reported in Tables 2 and 3 gives an idea of the intrinsic uncertainty in the interpolation procedures. As temperature increased, while A^{∞}_{C2} decreased, γ remained approximately constant. The linear plot of $-dA_{C2}/dt$ versus $10^{-A'_{C2}}$ (Eq. (12)) gave $\varepsilon_{C2}\Phi_{-C2}I^0$ from both the intercept and slope. An example of data treatment according to Eq. (12), to determine the product $\Phi_{-C2}\varepsilon_{C2}$, is shown in Fig. 6. The excellent correspondence (within 0.5%) of the two values at each temperature supports the reliability of the results; the higher temperature data are more uncertain due to the very low absorbance at the analysis wavelength. The Φ_{-C2} value could not be determined since ε_{C2} is unknown, however, since molar absorption coefficients of coloured forms generally range from 10^4 to 10^5 dm^3 mol^{-1} cm^{-1}, the photobleaching quantum yield (Φ_{-C2}) is expected to be smaller than 0.1.

Table 3
Photobleaching parameters for **3**[a]

T (K)	A^{∞}_{C2}	γ (s^{-1})	Intercept	Slope	$\Phi_{-C2}\varepsilon_{C2}$ (dm^3 mol^{-1} cm^{-1})
300	0.0078	0.0020	0.00083	0.00082	(980)
295	0.0081	0.0029	0.00121	0.00121	1430
290	0.0160	0.00335	0.00145	0.00148	1720
285	0.0290	0.0024	0.00106	0.00108	1270
280	0.0410	0.0021	0.00094	0.00097	1130
275	0.0480	0.0015	0.00066	0.00068	800

[a] A^{∞}_{C2} and γ are the fitting parameters (Eq. (11)); intercept, slope and $\Phi_{-C2}\varepsilon_{C2}$ were obtained by graphical treatment according to Eq. (12).

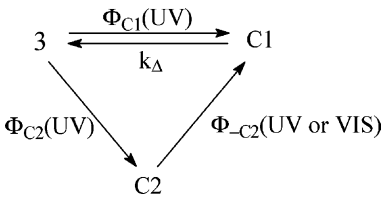

Scheme 3.

Photobleaching was found to be temperature dependent. To obtain a rough evaluation of the activation energy, an Arrhenius-type relationship (Eq. (14)) [12] was used, assuming the maximum $\varepsilon_{C2}\Phi_{-C2}$ as limiting value and excluding the highest temperature values due to their uncertainty.

$$-\ln\left\{[\Phi_{-C2}/(\Phi_{-C2})_{exp}]-1\right\} = -E_a/RT + \text{constant} \quad (14)$$

From the plot of $-\ln[\Phi_{-C2}/(\Phi_{-C2})_{exp}-1]$ versus $1/T$ ($\rho = 0.98$), an activation energy $E_a = 76\,\text{kJ mol}^{-1}$ was found. This value is close to that determined for the thermal bleaching of C1. This suggests the hypothesis that the thermal barrier to the C1 $\rightarrow$ ***3*** closure constitutes a bottleneck to the C2 $\rightarrow$ ***3*** overall process. From the foregoing it is proposed that photocoloration and bleaching of **3** involve two parallel photochemical steps that independently form C1 and C2 (Scheme 3). Since the molar absorption coefficients of the C1 and C2 isomers are expected not to be much different, the yield of C1 is greater than that of C2. The bleaching of C1 occurs thermally, that of C2 by irradiation with visible light, through C1 formation.

Based on a photokinetic method already developed [11], the fitting parameters obtained from the colour forming kinetics are related to kinetic parameters of the system, such as quantum yields and molar absorption coefficients. In particular, for a photochromic system yielding two photoproducts, C1 and C2, in parallel steps, the sum of the products of the exponential (α and β) and corresponding pre-exponential (B and C) factors is related to the quantum yields and molar absorption coefficients of C1 and C2 (Eq. (15)), independently of temperature and other steps that might occur in sequence or in parallel.

$$\alpha B + \beta C = I^0 F \varepsilon_{BiPh}[\mathbf{3}]_0(\varepsilon_{C1}\Phi_{C1} + \varepsilon_{C2}\Phi_{C2}) \quad (15)$$

In contrast, the individual pre-exponential factors depend on the kinetic parameters that govern the overall reaction mechanism. For Scheme 3, they are given by Eq. (16).

$$\alpha = I^0 F \varepsilon_{BiPh}[\Phi_{C1} + (\varepsilon_{C2}/\varepsilon_{C1})\Phi_{C2}] + k_\Delta$$
$$\beta = I^0 F \varepsilon_{BiPh}[(\varepsilon_{C1}/\varepsilon_{C2})(\Phi_{C1} - \Phi_{-C2}) + \Phi_{C2} + \Phi_{-C2}] \quad (16)$$

Based on Scheme 3, α should be temperature dependent while β should not, as was experimentally found. While it is intriguing to use Eq. (16) to extract the reaction parameters, Eq. (15) indicates that the $\alpha B + \beta C$ sum, that was expected and found to be temperature independent, can be used to determine the $\varepsilon_{C1}\Phi_{C1} + \varepsilon_{C2}\Phi_{C2}$ sum (Table 2, last column). By comparing this value ($6100 \pm 300\,\text{dm}^3\,\text{mol}^{-1}\,\text{cm}^{-1}$) with the $\varepsilon_{C1}\Phi_{C1}$ value obtained from the initial rate method ($4900\,\text{dm}^3\,\text{mol}^{-1}\,\text{cm}^{-1}$), it can be deduced, by subtraction, that $\varepsilon_{C2}\Phi_{C2}$ is $1200 \pm 300\,\text{dm}^3\,\text{mol}^{-1}\,\text{cm}^{-1}$. As for the photobleaching (vide supra), this small value is related to the low quantum yield (<0.1), in agreement with our hypotheses.

3.4. Compound *4*

The absorption spectrum of the colourless form of compound **4** shows a partially resolved structure with maxima at 320 and 349 nm, $\varepsilon_{max} = 17,750$ and $15{,}950\,\text{dm}^3\,\text{mol}^{-1}\,\text{cm}^{-1}$, respectively. The spectrum, if compared with that of the single molecule, indicates that the ester bridge has more remarkable effects on the spectral patterns than the ethane bridge, as expected. Photocolouration of a $2 \times 10^{-5}\,\text{mol dm}^{-3}$ toluene solution was carried out by irradiating at an isosbestic point (366 nm). The spectrum of the colourless form and that of the photostationary state coloured solution are shown in Fig. 7. The colour-forming kinetics, followed at $\lambda_{max} = 443$ nm, was found to be described by a bi-exponential function (Eq. (10)). The fitting parameters (B, C, α, β) are reported in Table 4. It can be observed that the apparent rate parameters, α and β, differ by about 1 order of magnitude; both decreased with decreasing temperature.

In contrast with the other three molecules, the thermal kinetics was described at the best by a bi-exponential function, Eq. (17). However, similarly to **3**, the thermal bleaching left a residual absorption (A^{∞}_{C3}), that was even smaller than for **3**, about 6–8% of the total absorption at the photostationary state, and substantially independent of temperature. The parameters (B', C', k_1, k_2 and A^{∞}_{C3}), resulting from non-linear fitting procedures, are reported in Table 5.

$$A = B'\,e^{-k_1 t} + C'\,e^{-k_2 t} + A^{\infty}_{C3} \quad (17)$$

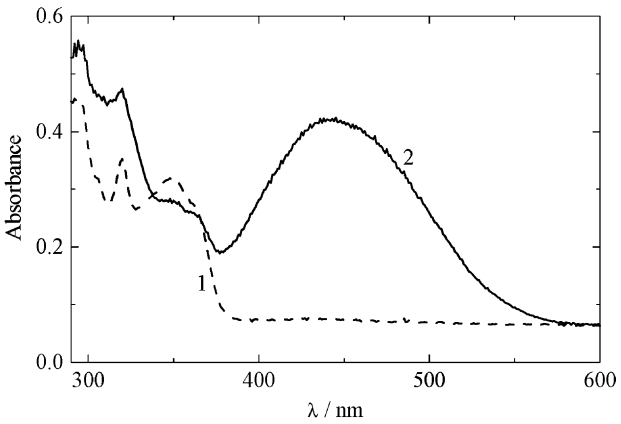

Fig. 7. Absorption spectra of **4** before irradiation (1) and at the photostationary state (2) in toluene; $3 \times 10^{-5}\,\text{mol dm}^{-3}$, at 265 K.

Table 4
Fitting parameters (B, C, α, β) of the colour-forming process of **4** in 2×10^{-5} mol dm^{-3} toluene solution obtained from Eq. (10) at various temperatures[a]

T (K)	B	α (s^{-1})	C	β (s^{-1})	$(\Phi\varepsilon)_{\text{initial rate}}$ (dm^3 mol^{-1} cm^{-1})	$\varepsilon_{C1}\Phi_{C1} + \varepsilon_{C2}\Phi_{C2}$ (dm^3 mol^{-1}cm^{-1})	$\varepsilon_{C1}\Phi_{C1}$ (dm^3 mol^{-1} cm^{-1})
285	0.0514	0.00964	0.0555	0.0285	5600	7062	1462
280	0.084	0.00657	0.0893	0.0198	6000	7888	1888
275	0.1363	0.00561	0.0868	0.0173	5700	7892	2192
270	0.1844	0.00378	0.1030	0.0141	5400	7321	1921
265	0.2105	0.00285	0.1635	0.0099	5500	7526	2026

[a] $(\Phi\varepsilon)_{\text{initial rate}}$ was obtained from Eq. (8) and $\varepsilon_{C1}\Phi_{C1} + \varepsilon_{C2}\Phi_{C2}$ from Eq. (15).

Table 5
Fitting parameters (Eq. (17)) of the thermal bleaching of **4** (2×10^{-5} mol dm^{-3}) in toluene

T (K)	B'	C'	k_1 (s^{-1})	k_2 (s^{-1})	A^{∞}_{C3}
285	0.0702	0.0309	0.01100	0.0319	0.0058
280	0.1206	0.0378	0.00639	0.0224	0.0110
275	0.1675	0.0410	0.00412	0.0176	0.0187
270	0.2094	0.0472	0.00256	0.0132	0.0297
265	0.2772	0.0729	0.00144	0.0082	0.0228

As can be seen from the table, the major contribution to the bleaching is provided by the long-lived component C1, whose relative amount increases with decreasing temperature. The activation energies determined for the two thermal processes are 62.5 kJ mol^{-1} ($\rho = 0.999$) for the slow component and 41 kJ mol^{-1} ($\rho = 0.994$) for the faster one (Fig. 8). There is a meaningful difference also between the frequency factors, 3×10^9 and 1×10^6 s^{-1}, respectively, of the two thermal processes. The activation energy and frequency factor of the slow component have the values typical of chromenes (compare Tables 1 and 7). This suggests that k_1 may be coupled with the isomer that mainly contributes to photocoloration (C1). Another relevant point is that the thermal rate constants (k_1 and k_2) and the apparent photochemical rate constants (α and β) appear to be coupled, that is, the thermal processes govern the photocolouration.

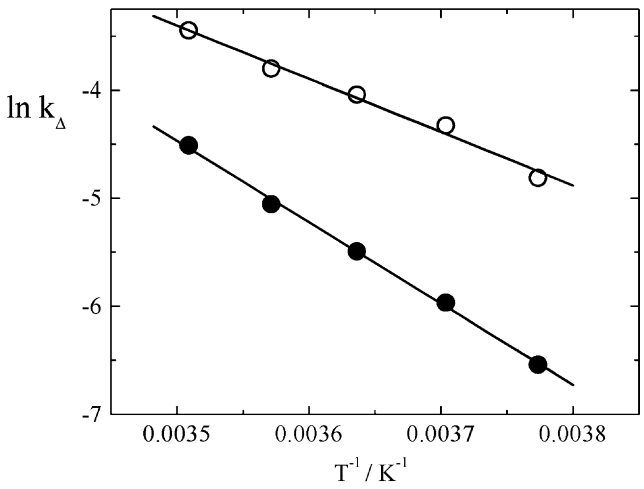

Fig. 8. Arrhenius plots for **4**: (●) slow thermal bleaching (k_1); (○) fast thermal bleaching (k_2).

Following a procedure analogous to that for **3**, the initial rate method yields $\varepsilon_{C1}\Phi_{C1} = 5600 \pm 300$ dm^3 mol^{-1} cm^{-1}, while Eq. (15) yields $\varepsilon_{C1}\Phi_{C1} + \varepsilon_{C2}\Phi_{C2} = 7500 \pm 300$ dm^3 mol^{-1} cm^{-1}. From where $\varepsilon_{C2}\Phi_{C2} = 1900$ dm^3 mol^{-1} cm^{-1} was obtained.

The residue A^{∞}_{C3} faded under irradiation with visible light. Photobleaching was carried out using 440 nm monochromatic light. The parameters $\varepsilon_{C3}\Phi_{-C3}$ and γ (Eq. (11b)) were determined as for **3**, the results are reported in Table 6. The $\varepsilon_{C3}\Phi_{-C3}$ values, as well as the γ-values, were constant at the highest temperatures but decreased at lower temperatures. The activation energy, roughly evaluated under the same hypotheses as for **3**, was found to be approximately 80 kJ mol^{-1}. This is a very rough number since it was determined from the three points at the lowest temperatures. Analogously to **3**, given the small $\Phi_{-C3}\varepsilon_{C3}$ value, the photobleaching quantum yield of C3 is surely very small.

To gain more insight into the complex photochromic mechanism of this compound, that implies formation of two thermally unstable (C1 and C2) and one thermally stable (C3) photoproducts, photocoloration was carried out at a temperature (200 K) low enough to reduce all thermally activated processes. Under these conditions, the system would reach a photostationary state which is thermally stable and substantially constituted by open form(s) only. The results obtained are illustrated in Figs. 9 and 10 where the spectral changes and kinetics upon UV irradiation, keeping the system in the dark and upon visible irradiation are shown. Irradiation with UV monochromatic light (366 nm) was carried out up to photostationary state attainment (bi-exponential colour-forming kinetics). The maximum of the colour band appeared at 455 nm, shifted to the red compared with that at higher temperatures (λ_{max}= 443 nm) (Table 7). This indicates that different product(s) were formed or that they

Table 6
Photobleaching parameters for **4**[a]

T (K)	A^{∞}_{C3}	γ (s^{-1})	Intercept	Slope	$\Phi_{-C3}\varepsilon_{C3}$
285	0.0065	0.00323	0.00121	0.00121	1330
280	0.0093	0.00299	0.00145	0.00148	1330
275	0.0157	0.00299	0.00106	0.00108	1370
270	0.0323	0.00185	0.00094	0.00097	880
265	0.0413	0.00135	0.00066	0.00068	650

[a] $A^{\infty}_{C3}$and γ are the fitting parameters (Eq. (11)); intercept, slope and $\Phi_{-C3}\varepsilon_{C3}$ were obtained by graphical treatment according to Eq. (12).

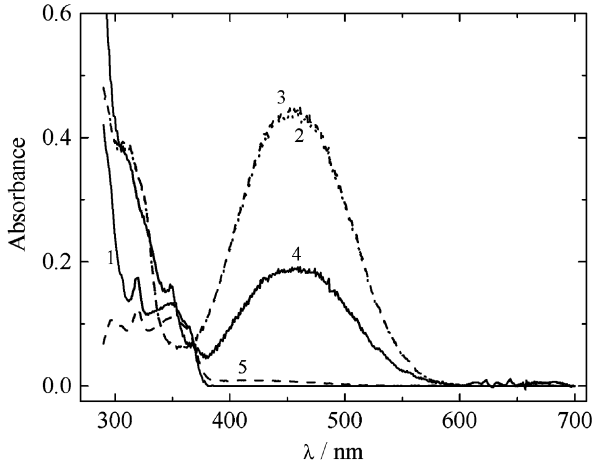

Fig. 9. Spectra of **4** in toluene (8×10^{-6} mol dm^{-3}) at 200 K: (1) before irradiation; (2) photostationary state under irradiation at 366 nm; (3) kept in the dark; (4) photostationary state under monochromatic irradiation at 455 nm; (5) after thermal equilibration at room temperature.

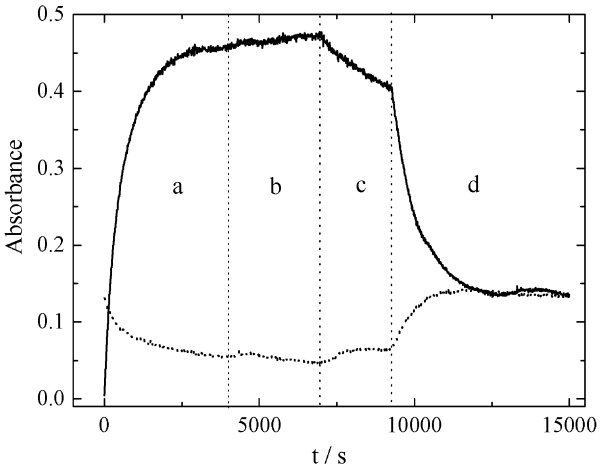

Fig. 10. Kinetic evolution of the absorbance of **4** in toluene (8×10^{-6} mol dm^{-3}) at 200 K, monitored at 455 nm (solid line) and 350 nm (dotted line): (a) under irradiation at 366 nm; (b) in the dark; (c) under monochromatic irradiation at 455 nm (band pass 16 nm); (d) under visible irradiation using larger (all open) monochromator slits.

were formed in different relative amounts. The photostationary solution, kept in the dark at 200 K (3000 s), did not show any spectral change: spectra 2 and 3 in Fig. 9 perfectly overlap. Only upon irradiation with visible light

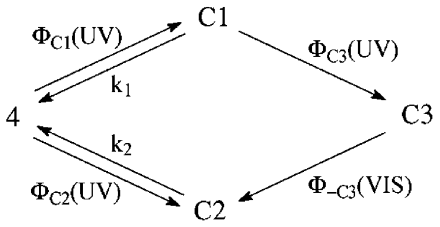

Scheme 4.

(455 nm), slow and partial photobleaching was observed ($\varepsilon_{C3}\Phi_{-C3} = 660\,\mathrm{dm^3\,mol^{-1}\,cm^{-1}}$) leading to a new photostationary state. The spectrum, while maintaining the principal maximum in the visible (λ_{max}= 455 nm), exhibited a new peak at 350 nm, that is, the partial decrease in the visible absorbance matched the absorbance increase at 350 nm (Figs. 9 and 10). On increasing temperature, the initial spectrum of the closed form was restored. The peak at 350 nm, characteristic of the species that was thermally and photochemically stable at 200 K and bleached at higher temperature, was not detected in the photostationary state mixtures obtained in the 265–285 K temperature range. However, it could have not been observed due to very low concentration. Based on the foregoing observations, a tentative reaction mechanism is proposed in Scheme 4.

Upon UV irradiation, **4** mainly gives C1 which thermally (k_1) back reconverts to the starting molecule, while C2 is produced at a minor extent due to both lower quantum yield and faster back reaction (k_2). The major product photochemically also gives a third species, C3. When temperature is not so low to stop the thermal processes, all species (**4**, C1–C3) are present at the photostationary state; when irradiation is discontinued C1 and C2 thermally bleach, while C3 only bleaches upon visible irradiation. At low temperature (200 K), the relative amounts of photostationary products, stable in the dark, are controlled by photochemistry and the solution contains mainly C3 (formed from C1) and C2 as a minor component. By visible irradiation C3 totally converts to C2. By increasing temperature the closed form is obtained, through the thermal process C2 → ***4***.

The assignment of the photoproduct structures is not easy. If C1–C3 are conformers or *cis–trans* isomers of the open form, it can be assumed that thermal activation is sufficient for promoting processes implying rotation around a single

Table 7
Spectral and kinetic parameters obtained from the photokinetic study of **3** and **4** in toluene solution

	3	**4**
λ_{max} (nm)	431	443
λ_{iso} (nm)	365	366
ε_{C1} (dm^3 mol^{-1} cm^{-1})	30100	
Φ_{C1}	0.20	
$k_{\Delta(280)}$ (s^{-1})	0.0041	0.0064 (k_1, slow process); 0.022 (k_2, fast process)
$k_{\Delta(298)}$ (s^{-1})	0.021	0.033 (slow); 0.065 (fast)
E_a (kJ mol^{-1})	64	62.5 (slow); 41 (fast)
A (s^{-1})	3.6×10^9	3×10^9; (slow); 1×10^6 (fast)

bond while light absorption is needed when rotation around a double bond is involved. An alternative/additional hypothesis could be that C1 and C2 are coloured forms with only one open chromene moiety, while C3 has both the chromene moieties open. The latter hypothesis would be supported by the magnitude of the ε-values: that of C3 is calculated from the UV photostationary state at 200 K, assuming total conversion ($\varepsilon_{C3} \sim 56,000\,dm^3\,mol^{-1}\,cm^{-1}$), while that of C2 can be obtained from the photostationary state reached after the visible bleaching ($\varepsilon_{C2} \sim 23,000\,dm^3\,mol^{-1}\,cm^{-1}$). By using these ε-values and the experimental $\Phi\varepsilon$-values, $\Phi_{C2} = 0.08$ and $\Phi_{-C3} = 0.01$ are obtained.

4. Conclusions

These results show that the presence of two photochromic moieties in the supermolecules investigated does not substantially change the reversible behaviour exhibited by the single components, contrary to what was previously found for supramolecular systems where the link between the two photochromes was an ethenic bridge [3,4]. However, there are some interesting features concerning chromaticity and the relative contribution of thermal and photochemical bleaching, that are different from those of the single molecules.

Compared to the single molecules, the absorption spectra of the coloured forms shift to the red at an extent that depends on the nature of the link. Colourability generally increases. Particularly interesting is the spectrum of the compound containing both chromene and spirooxazine moieties (**2**) that extends from 400 to 650 nm, covering almost all the visible region. This extended absorption results in a grey colour of the active form.

Reversibility is substantially complete. However, for two of the studied molecules (**1** and **2**), only thermal reversibility was detectable, while in chromene single molecules both thermal and photochemical reversibilities are generally present [12]. For the two systems that are thermo- and photo-reversible (**3** and **4**), the contribution of the photochemical process to the overall colour-fading is much smaller (about 10%) than for the single chromene (about 50%). For these two molecules the kinetic behaviour is quite complex and allows only tentative reaction mechanisms to be proposed.

Acknowledgements

The research of the group of Perugia was funded by the Ministero per l'Università e la Ricerca Scientifica e Tecnologica (Rome) and the University of Perugia in the framework of the Programmi di Ricerca di Interesse Nazionale (project: Mechanisms of Photoinduced Processes in Organized Systems). A grant from the Italian Consiglio Nazionale delle Ricerche (Rome) is also acknowledged (Progetto Finalizzato: "Materiali Speciali per Tecnologie Avanzate II")

References

[1] J.C. Crano, R.J. Guglielmetti, (Eds.), Organic Photochromic and Thermochromic Compounds, Vols. 1 and 2, Plenum Press, New York, 1998–1999.
[2] R. Guglielmetti, in: H. Dürr, H. Bouas-Laurent (Eds.), Photochromism: Molecules and Systems, Elsevier, Amsterdam, p. 314, 1990 (Chapter 8).
[3] F. Ortica, D. Levi, P. Brun, R. Guglielmetti, U. Mazzucato, G. Favaro, J. Photochem. Photobiol. A: Chem. 138 (2001) 123.
[4] F. Ortica, D. Levi, P. Brun, R. Guglielmetti, U. Mazzucato, G. Favaro, J. Photochem. Photobiol. A: Chem. 139 (2001) 133.
[5] D. Levi, Ph.D. Thesis, Université de la Méditerranée, Marseille Luminy, France, 2000.
[6] G. Ottavi, G. Favaro, V. Malatesta, J. Photochem. Photobiol. A: Chem. 115 (1998) 123.
[7] B. Van Gemert, in: J.C. Crano, R.J. Guglielmetti (Eds.), Organic Photochromic and Thermochromic Compounds, Vol. 1, Plenum Press, New York, p. 111, 1998 (Chapter 3).
[8] F. Wilkinson, J. Hobley, M. Naftaly, J. Chem. Soc., Faraday Trans. 88 (1992) 1511.
[9] G. Favaro, F. Masetti, U. Mazzucato, G. Ottavi, P. Allegrini, V. Malatesta, J. Chem. Soc., Faraday Trans. 90 (1994) 333.
[10] V. Pimienta, D. Lavabre, G. Levy, A. Samat, R. Guglielmetti, J.C. Micheau, J. Phys. Chem. 100 (1996) 4485.
[11] G. Ottavi, F. Ortica, G. Favaro, Int. J. Chem. Kinet. 31 (1999) 303.
[12] G. Favaro, A. Romani, R.S. Becker, Photochem. Photobiol. 72 (2000) 632.
[13] F. Ortica, G. Favaro, J. Phys. Chem. B 104 (2000) 12179.
[14] G. Favaro, V. Malatesta, U. Mazzucato, G. Ottavi, A. Romani, J. Photochem. Photobiol. A: Chem. 87 (1995) 235.
[15] J.L. Pozzo, A. Samat, R. Guglielmetti, D. De Keukeleire, J. Chem. Soc., Perkin Trans. 2 (1993) 1327.
[16] P. Laréginie, V. Lokshin, A. Samat, R. Guglielmetti, G. Pèpe, J. Chem. Soc., Perkin Trans. 2 (1996) 107.
[17] A. Kellmann, F. Tfibel, R. Dubest, P. Levoir, J. Aubard, E. Pottier, R. Guglielmetti, J. Photochem. Photobiol. A: Chem. 49 (1989) 63.
[18] N.Y.C. Chu, Can. J. Chem. 61 (1983) 300.